

# The effects of deposition rate on the structural and electrical properties of ZnO:Al films deposited on (11 $\bar{2}$ 0) oriented sapphire substrates

Yasuhiro Igasaki and Hiromi Saito

Research Institute of Electronics, Shizuoka University, Johoku 3-5-1, Hamamatsu 432, Japan

(Received 3 May 1991; accepted for publication 26 June 1991)

Aluminum doped zinc oxide (ZnO:Al) films were deposited on (11 $\bar{2}$ 0) oriented sapphire substrates heated to 200 °C with a radio-frequency (rf) power ranging from 25 to 170 W for a deposition rate in the range 0.7–27.4 nm min<sup>-1</sup> by rf-magnetron sputtering from a ZnO target mixed with Al<sub>2</sub>O<sub>3</sub> of 2 wt. %. All of the films deposited were (0001) oriented single-crystalline films with an internal stress. The stress was increased and degraded the crystallinity of the epitaxial film as a deposition rate was increased, and thus the Hall mobility and the resistivity of the film were, respectively, decreased and increased. However, the resistivities obtained were in the range about 1.4–3.0 × 10<sup>-4</sup> Ω cm, the values comparable to those for indium tin oxide film presently used as a transparent electrode.

## I. INTRODUCTION

Recently, aluminum-doped zinc-oxide (ZnO:Al) films have been actively investigated as a transparent conducting material in place of indium tin oxide (ITO).<sup>1–7</sup> However, the values of electrical resistivities reported were relatively divergent. The electrical properties of ZnO:Al films are so affected by adsorption of oxygen on the surfaces of ZnO:Al crystallites<sup>8</sup> that values for their electrical resistivity differ with morphological structure of each film. Therefore, in order to know the attainable value for the electrical resistivity of ZnO:Al films, the electrical resistivity of a single-crystal film should be measured beforehand. Following the reports by Paradis and Shuskus,<sup>9</sup> Mu-shiang Wu *et al.*<sup>10</sup> and Mitsuyu *et al.*,<sup>11</sup> we used the sapphire (11 $\bar{2}$ 0) plane in order to grow a single-crystal ZnO:Al film on a sapphire substrate at lower temperatures.

Krikorian and Sneed have established that the three most important parameters which determine epitaxial growth in sputtering for a given material and substrate are substrate temperature, deposition rate, and background pressure.<sup>12</sup> In a previous study,<sup>13</sup> we investigated the substrate temperature dependence of the structural and electrical properties of ZnO:Al films deposited on (11 $\bar{2}$ 0) sapphire substrates and obtained the following results:

(1) The films deposited on a substrate heated up to 350 °C with a deposition rate in the range 1.7–3.1 nm min<sup>-1</sup> were (0001) oriented single-crystal films.

(2) A resistivity of about 1.5 × 10<sup>-4</sup> Ω cm was obtained with films grown at 150 °C.

(3) The resistivities of the films were gradually increased over the substrate temperature range from 200 to 350 °C and the increase in resistivity was ascribed mainly to decrease in carrier concentrations.

(4) The films deposited at 200 °C showed the maximum value for the Hall mobility. In this paper, we report the deposition-rate dependence of the structural and electrical properties, especially the Hall mobility, of the ZnO:Al films grown on a sapphire (11 $\bar{2}$ 0) surface. A variation in deposition rate was obtained by changing the radio-frequency (rf) power.

## II. EXPERIMENT

There are a few parameters which determine deposition rate in sputtering such as sputtering power, sputtering gas pressure, distance between substrate and target, and so on. In the present study, we changed sputtering power in order to vary the deposition rate.

ZnO:Al films were prepared by rf-magnetron sputtering. The apparatus used was a NEVA type FP 45 rf-sputtering system modified for magnetron sputtering. A sintered disk of ZnO (purity, 99.99%) mixed with 2 wt. % Al<sub>2</sub>O<sub>3</sub> (purity, 99.99%), 125 mm in diameter, was used as a target. A substrate heating device was mounted on a water-cooled anode. The distance between target and substrate was about 9 cm. The residual gas and the sputtering gas were monitored with a *B-A* type ionization gauge and a capacitance manometer, respectively. Details of the apparatus have been reported elsewhere.<sup>14</sup>

Before deposition, the sapphire substrates were ultrasonically cleaned in a weak alkaline cleaning solution provided by Furuuchi Chemical Laboratory, in acetone and finally in methyl alcohol. Sputtering was carried out at a pressure of 1.33 Pa in an argon gas with an rf power ranging from 25 to 170 W. The deposition rate in this study was in the range 0.7–27.4 nm min<sup>-1</sup>. Figure 1 shows the deposition rate as a function of rf power. The deposition rates at rf powers larger than 40 W increase in proportion to the rf power to about the 1.6 power. Deviation from the relation at lower powers is perhaps ascribed to a reading precision for the power meters. After a presputtering of 10 min, films were deposited onto sapphire (10 × 10 mm and 5 × 5 mm) and quartz (10 × 10 mm) substrates heated to 200 °C. The deposition time was 20–310 min for a final thickness in the range 83–670 nm. This film thickness was determined with a DEKTAK surface roughness detector.

The crystal structure of ZnO:Al film was studied by x-ray diffraction using CuKα line with a RIGAKU type RAD-IIA and by electron diffraction with a JEOL type JEM-100U. A JEOL type JSM-T330A scanning microscope equipped with a wavelength dispersive x-ray spectroscopy (WDS) JXA-840AP was used for the observation of

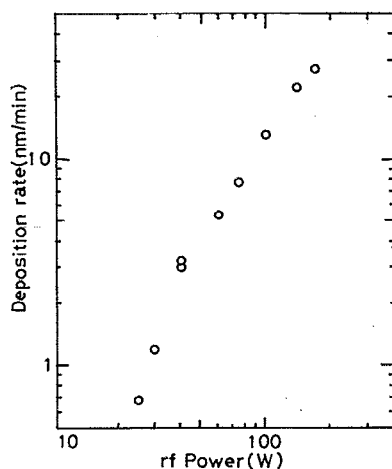


FIG. 1. Deposition rate as a function of rf power. Substrate temperature was 200 °C. The distance between target and substrate was about 9 cm.

surface morphology and for the estimation of aluminum content. A WDS analysis was done using ZnO:Al films deposited on quartz substrates.

The electrical resistivity  $\rho$  and the Hall coefficient  $R_H$  were measured using the van der Pauw method. An electric current  $I$  ranging from 0.1 to 1.0 mA at 0.1 mA intervals was applied through electrodes and each potential difference  $V$  between the electrodes was measured. The resistivity was calculated from the  $V$  vs  $I$  curve using the least-squares method. The Hall voltage was measured under an electric and a magnetic field and then reversed fields; the current and the magnetic field used were, respectively, 10 mA and 3000 G. The carrier concentration  $N$  and the Hall mobility  $\mu$  were calculated from the electrical resistivity and the Hall coefficient using the following relations:

$$\rho = 1/Ne\mu, \quad (1)$$

$$R_H = 1/Ne. \quad (2)$$

The optical transmittance for ZnO:Al films deposited on quartz substrates was measured at room temperature with unpolarized light in the spectral range from 300 to 2600 nm.

### III. RESULTS AND DISCUSSION

#### A. Al content in ZnO:Al films

The aluminum dopant concentration is considered to be by far the most important parameter to affect the electrical properties of ZnO:Al single-crystal films. The Al/Zn ratio was determined using films deposited on quartz substrates by WDS analysis. Standard samples used were Zn and Al metals. The acceleration voltage and the take-off angle were 15 kV and 35°, respectively. The measured value, which was the average of three measurements, was corrected using the ZAF method. The value for thick films (1500 nm) regarded as bulk materials agreed within experimental errors with those for thinner films prepared under the same conditions.

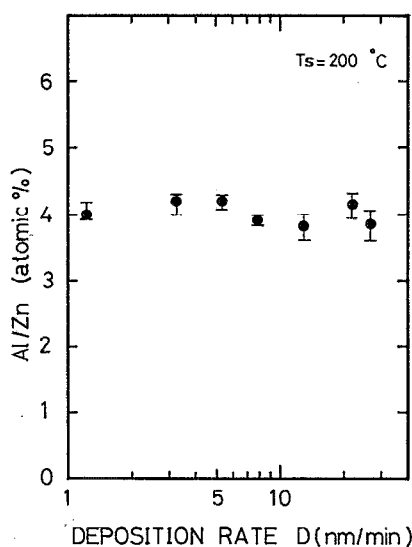


FIG. 2. Al/Zn ratio (at. %) in ZnO:Al films as a function of deposition rate for films deposited on quartz substrates analyzed by WDS. Error bars show deviations of measurement values at three different points.

Figure 2 shows the Al/Zn ratio in atomic percent as a function of deposition rate. Measurements were done at three different points on a sample. The error bars represent the divergence in measurement values and the solid circles are the average values. The Al/Zn ratio in films grown at a deposition rate in the range 1.2–27.4 nm min<sup>-1</sup> is about 4 at.% and almost independent of deposition rate. The specific gravity of ZnO crystals is 5.72 g cm<sup>-3</sup>, corresponding to 4.2×10<sup>22</sup> molecules per cm<sup>3</sup>.<sup>15</sup> Therefore, the aluminum content in the ZnO:Al films is roughly estimated to be 1.6×10<sup>21</sup> cm<sup>-3</sup>.

#### B. Electrical properties

Figure 3 shows the electrical properties such as resistivity  $\rho$ , carrier concentration  $N$ , and the Hall mobility  $\mu$  of ZnO:Al films grown on (11 $\bar{2}$ 0) oriented sapphire substrates as a function of deposition rate. As a deposition rate was increased, the resistivity  $\rho$  was increased from the minimum value of about 1.4×10<sup>-4</sup> Ω cm at 1.2 nm min<sup>-1</sup> to the maximum value of about 3.0×10<sup>-4</sup> Ω cm at 22.3 nm min<sup>-1</sup>. However, the resistivities of these films are less than 3×10<sup>-4</sup> Ω cm and are comparable to the resistivity of ITO film. Therefore, even if high-rate deposition is required in practice, the ZnO:Al films with resistivities low enough to be used as transparent conductors can be easily prepared.

The resistivity  $\rho$  is proportional to the reciprocal of the product of the carrier concentration  $N$  and the mobility  $\mu$ . Therefore, the change in resistivity with deposition rates shown in Fig. 3 is ascribed to the change in  $N$  and/or  $\mu$  which are characteristic parameters reflecting the film structure and/or the impurity contents.

As shown in Fig. 3, as the deposition rate is increased, the carrier concentration  $N$  is gradually decreased from 1.3×10<sup>21</sup> cm<sup>-3</sup> at 1.2 nm min<sup>-1</sup> to 1.1×10<sup>21</sup> at 27.4 nm

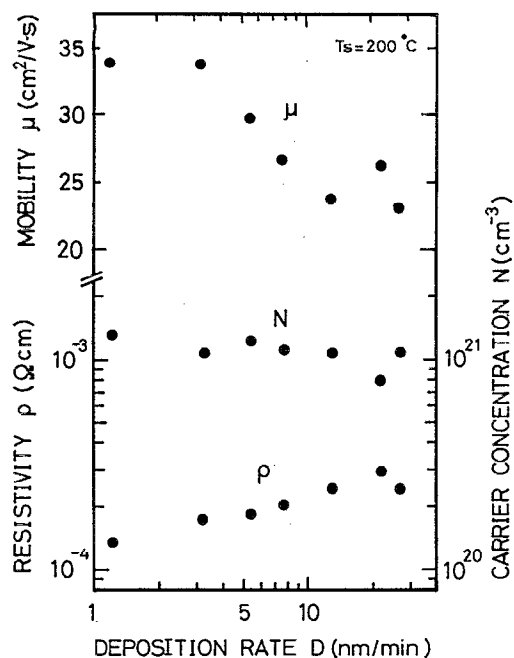


FIG. 3. The Hall mobility  $\mu$ , carrier concentration  $N$  and resistivity  $\rho$  as a function of deposition rate.

$\text{min}^{-1}$ . However, as shown in Fig. 2, the aluminum content is almost independent of the deposition rates. Furthermore, the carriers in part may be excited from native defects such as interstitial zinc atoms and/or oxygen vacancies.<sup>13</sup> Also native defects are expected to increase with rf power when a sintered ZnO target was sputtered with pure argon.<sup>16</sup> Therefore, if the carriers shown in Fig. 3 represent all of the free electrons excited from the aluminum atoms and native defects, we must recognize the unlikely result that the number of aluminum atoms and/or native defects, which act as donors among them, varies with growth rate.

On the other hand, because the surface of ZnO is chemically active, oxygen chemisorbed on ZnO surfaces accepts an electron from occupied conduction band states and then reduces the carrier concentration in the ZnO.<sup>17</sup> Therefore, as real surface area is increased, the carrier concentration is decreased. Namely, in the present case, it should be considered that the real surface area was increased as the deposition rate was increased, thus increasing a fraction of free electrons trapped by oxygens chemisorbed on the surface of ZnO:Al crystallites.

As shown in Fig. 3, the Hall mobility  $\mu$  also decreases with a deposition rate. The mobility of carriers is closely related to the macroscopic and/or microscopic imperfections in the films. The macroscopic imperfections include grain boundaries, internal stress, and surface roughness which can be observed from the x-ray diffraction spectrum or SEM photographs, and the microscopic imperfections include the ionized donors and/or the neutral impurity atoms. Especially in ZnO, a surface barrier made by the chemisorption of oxygen onto the surface of crystallites considerably reduces the mobility of carriers.<sup>17</sup> Therefore,

the grain boundary is considered to be the most effective of the carrier mobility.

The mobility of carriers in thinner ZnO:Al films with a smooth surface strongly depended on film thickness and saturated at a thickness of about 300 nm.<sup>13</sup> Namely, it could be considered that the thickness dependence of the mobility in ZnO:Al epitaxial films was mainly ascribed to a change with film thicknesses in the concentration of the scattering centers for the carriers such as lattice strains and dislocations caused by the lattice mismatch between the film and the substrate. The mobility in the film with a thickness over about 300 nm was mainly decided by the concentration of point defects such as substitutional aluminum atoms and native defects.<sup>18</sup> However, the mobilities in the films deposited at higher rates shown in Fig. 3, although their thicknesses are in the range 383–670 nm and considered to be enough for the effect of lattice mismatch on the mobility to be neglected, are less than the saturated values for the films grown at lower deposition rates. This means that the concentration of the point defects was increased with the increasing deposition rate, and/or that another scattering center such as grain-boundary was introduced to the epitaxial film deposited at higher rates.

Thus, it can be concluded that in the present case, the number of trapping centers affecting the carrier concentration and the number of scattering centers affecting the mobility of carriers were increased with deposition rate, and that as a result, the carrier concentration  $N$ , the Hall mobility  $\mu$  were decreased and the resistivity  $\rho$  was increased with the deposition rate as shown in Fig. 3.

### C. Structural properties

In order to explain the dependence of the electrical properties on deposition rate, we investigated the changes in structural characteristics of films such as crystal structure and surface morphology. Reflection electron diffraction (RED) and x-ray diffraction (XRD) were used to estimate the crystallinity and epitaxial relationship between the film and the substrate. Scanning electron microscopy (SEM) was used for observation of the surface morphology.

Figure 4 shows the XRD patterns from ZnO:Al films deposited on sapphire (11 $\bar{2}$ 0) substrates heated to 200 °C with a deposition rate in the range 1.2–27.4 nm min<sup>-1</sup>. As shown in Fig. 4, XRD patterns from the films consist of the only (0002) peak of ZnO. This indicates that all of the ZnO:Al films grown on sapphire (11 $\bar{2}$ 0) substrates heated to 200 °C consist of the (0001) oriented ZnO:Al crystallites regardless of the deposition rate.

Figure 5 shows RED patterns from ZnO:Al films deposited on 5×5-mm sapphire substrates with the lowest and the highest rate as representative of entire rate region. Films deposited with the other rate showed the same patterns. RED patterns remained unchanged throughout the scan over the entire surface area. Each pattern shown in Figs. 5(a) or 5(b) was found to repeat every 60°, and the patterns alternated every 30° as the film was rotated in the beam. This is the type of behavior expected from a crystal with a sixfold symmetry. Therefore, two kinds of patterns

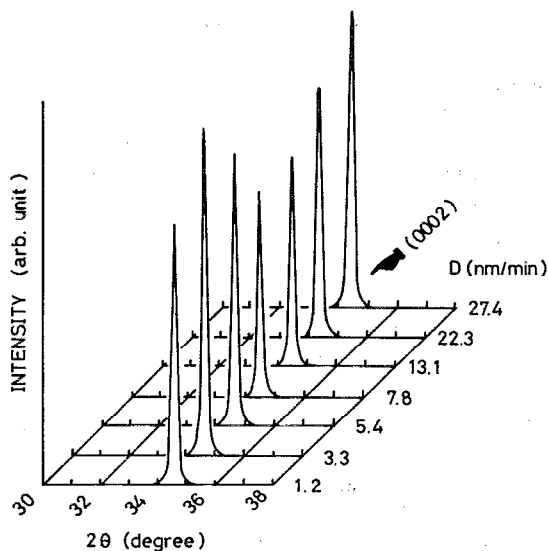
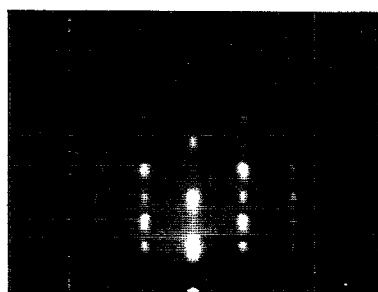
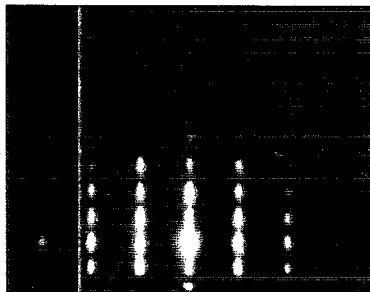


FIG. 4. X-ray diffraction patterns from ZnO:Al films deposited on the (1120) oriented sapphire substrate heated to 200 °C with a deposition rate  $D$ .

(a) and (b) correspond to the diffraction patterns of the two major zones which are perpendicular to the basal plane. The incident-beam directions were parallel to (a)  $[1\bar{2}10]$  and (b)  $[10\bar{1}0]$  directions, respectively. From these



$D = 0.7 \text{ nm/min}$



$27.4 \text{ nm/min}$



$D = 0.7 \text{ nm/min}$



$27.4 \text{ nm/min}$

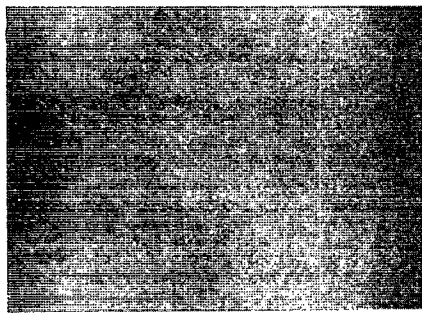
FIG. 5. RED patterns from ZnO:Al films on (1120) oriented sapphire substrates heated to 200 °C with a deposition rate  $D$ . The incident beam directions were parallel to (a)  $[1\bar{2}10]$  and (b)  $[10\bar{1}0]$  directions, respectively. Each pattern was found to repeat every 60°, and the patterns alternated every 30° as the film was rotated in the beam.

results, we can conclude that films deposited on (1120) sapphire substrates heated to 200 °C with a deposition rate ranging from 0.7 to 27.4 nm min<sup>-1</sup> are (0001) oriented ZnO:Al single-crystal films.

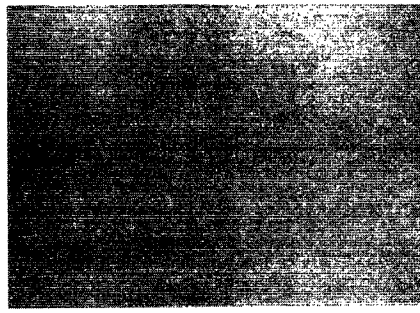
Figure 6 represents SEM photographs of the same films shown in Fig. 5. As shown in the figure the surfaces of the films, except a film deposited at 3.3 nm min<sup>-1</sup>, were relatively smooth, and a correlation between the surface morphology and the deposition rate or the Hall mobility was not found.

Figure 7 shows some characteristic parameters given by the XRD peak from ZnO (0002) plane as a function of deposition rate. The diffraction angle  $2\theta$ , is in the range 34.34°–34.61°. The values of  $2\theta$  seem to decrease as the deposition rate is increased. The value for the film deposited with about 13 nm min<sup>-1</sup> is nearly equal to the value of 34.47° for bulk materials (shown by a broken line in Fig. 7).

In general, when the network spacing of atoms composing the substrate surface is larger than that of the epitaxial film, a tensile stress is present near the interface of the film. As a result, the lattice constant vertical to a growing plane of the film is shorten in comparison with the value for bulk material and the  $2\theta$  moves to higher angles. The reverse is also true. Therefore, the change in  $2\theta$  with a deposition rate shown in Fig. 7 implies that the stress in films changes from tension to compression as the deposi-



$D=0.7 \text{ nm/min}$



$27.4 \text{ nm/min}$

FIG. 6. SEM photographs of ZnO:Al films deposited on (11 $\bar{2}$ 0) sapphire substrates heated to 200 °C with a deposition rate  $D$ . The scale bar is 1  $\mu\text{m}$ .

tion rate is increased. However, such a phenomenon in the epitaxial film is considered to be unreasonable because the network spacing of atoms at the interface region of the epitaxial films should be decided by the spacing of atoms composing the substrate surface.

We already reported<sup>13,18</sup> that the  $2\theta$  for (0001) diffraction from ZnO:Al films deposited on (11 $\bar{2}$ 0) oriented sapphire substrates was increased with substrate temperatures or with film thicknesses but the divergence of the values for  $2\theta$  was ascribed to the experimental errors because the absolute values for deviation of  $2\theta$  from the value for bulk material was very small. However, the variation of  $2\theta$  versus substrate temperature or film thickness was as relatively systematic as that versus deposition rate shown in Fig. 7. Therefore, we should correspondingly consider the variation of  $2\theta$  versus these parameters to the change in the structural properties.

When the stress is present in an epitaxial film, the internal energy of the film is increased as the film thickness

is increased. Therefore, if the growth rate is as low as the film is grown in equilibrium, the film may grow introducing dislocations to liberate the stress and to suppress the increase in the internal energy with the increasing film thickness. As a result, the lattice constant of the film can be expected to approach the value for bulk material as the film thickness is increased. Namely, provided that the network spacing of atoms at the substrate surface is smaller than that of overgrowth,  $2\theta$  for the growing plane of the film varies from lower angles to higher angles with the increasing film thickness and reaches the value for the bulk single crystal. Such a variation of  $2\theta$  coincides with the variation of  $2\theta$  for the (0001) plane of ZnO:Al films deposited on the (11 $\bar{2}$ 0) oriented sapphire substrates as a function of film thickness.<sup>18</sup>

On the contrary, in the case of the variation of  $2\theta$  versus substrate temperature, the observed stress change from compression to tension with the increasing substrate temperature appeared unreasonable.<sup>13</sup> Therefore, in the case of the substrate temperature dependence or the deposition rate dependence, we tentatively examined our data on the assumption that the maximum value for  $2\theta$  could be regarded as the value for the bulk within experimental errors. Furthermore, it is not so unreasonable for us to grant that interfacial stress is liberated in a relatively early stage of film growth at higher substrate temperatures and the stress remains in considerably thicker films grown with higher deposition rates. Namely, if we accept the above mentioned assumption, the higher a substrate temperature is and the smaller a deposition rate is at the earlier stage of film growth, the lattice constant of the film can reach the value for bulk material, and thus the deposition rate dependence and the substrate temperature dependence of  $2\theta$  observed can be considered to be reasonable.

The relatively large values for the standard deviation  $\sigma$  of the rocking curve on (0002) diffraction and half-widths (FWHM) of (0002) diffraction are not due to the intrinsic properties of films, but to the measuring system. Because those values for (11 $\bar{2}$ 0) diffraction ( $2\theta = 37.81^\circ$ ) from the substrate were 0.5° and 0.18°, respectively. However, the increase in  $\sigma$  at deposition rates more than 5.4 nm min<sup>-1</sup> should be considered to reflect the change in the crystallinity of the film. As discussed above, the interfacial stress remains in considerably thicker film grown at higher dep-

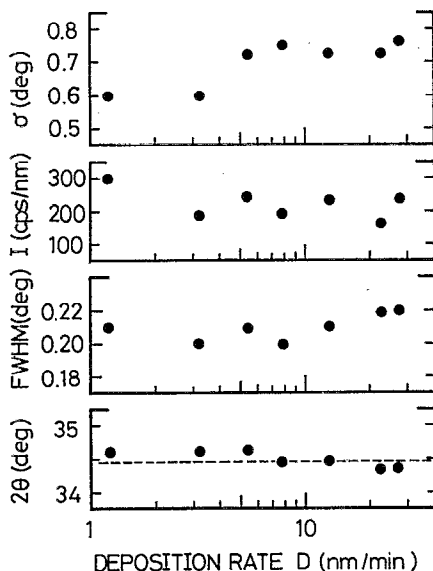


FIG. 7. Characteristic parameters, i.e., the diffraction angle  $2\theta$ , the half-width FWHM, and the intensity  $I$  of x-ray diffraction peak, and the standard deviation  $\sigma$  of the rocking curve from (0001) oriented ZnO:Al crystallites, as a function of deposition rate.

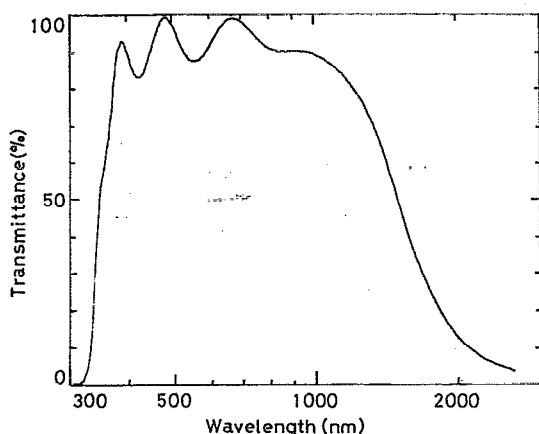


FIG. 8. Representative transmission spectrum of ZnO:Al film. The film measured was deposited on a quartz substrate heated to 200 °C at 13.1 nm min<sup>-1</sup>. The film thickness was about 390 nm.

osition rates and as a result, the film is expected to be divided into a mosaic structure in order to suppress the increase in the internal energy in the film. Because the mosaic structure is composed of many blocks with a narrow distribution of orientation and/or lattice constant,<sup>19</sup> it is considered that the  $\sigma$  and the full width at half maximum (FWHM) for the film with a mosaic structure is larger than the value for the film with a bulk structure. However, as shown in Fig. 7, FWHM seems to be slightly increased with the increasing deposition rate, but also the change can be regarded as within experimental errors. This may be the reason why FWHM is not so sensitive to the structural change as  $\sigma$  in our measurement system.

As discussed above, by analyzing the experimental results on the basis of the assumption that the network spacing of atoms in the substrate surface is smaller than that of the epitaxial film, we showed that the decrease in the Hall mobility with the increasing deposition rate was ascribed to the structural change of the film caused by the interfacial stress, reflected on the characteristic parameters of XRD peak. Furthermore, the change in film structure from a laminar structure to a mosaic structure leads to an increase in real surface area. Therefore, the formation of mosaics at higher deposition rates decreases the carrier concentration as well as the Hall mobility. This is analogous to the dependence of electrical properties on the deposition rate shown in Fig. 3.

Thus, we could correspondingly explain the electrical properties as a function of deposition rate to the structural change reflected on the characteristic parameters of XRD. However, further discussion needs more detailed analysis of the film structure, for example, XRD measurement using completely monochromated x ray.

#### D. Optical transmittance

Figure 8 gives a representative transmission spectrum from a ZnO:Al film deposited on a quartz substrate heated to 200 °C with a deposition rate of 13.1 nm min<sup>-1</sup>. The film thickness was 390 nm.

As shown in Fig. 8, the film has an average transmittance of about 90% with oscillatory character due to interference effects in the wavelength range of 400–1100 nm. A decrease in the transmission in the near-IR region is a result of free carrier absorption. This result was quite similar to those of other films. Therefore, these films can be used as transparent conducting films in the visible light range.

#### IV. CONCLUSION

ZnO:Al films were deposited on the (11 $\bar{2}$ 0) oriented sapphire substrates heated to 200 °C with a deposition rate ranging from 0.7–27.4 nm min<sup>-1</sup> by rf-magnetron sputtering from a sintered ZnO disk mixed with 2-wt.% Al<sub>2</sub>O<sub>3</sub>. From x-ray diffraction and electron diffraction measurements, it was found that the films were (0001) oriented single-crystal films. Furthermore, SEM observation revealed that the surfaces of films were relatively smooth and correlations between the surface morphology and the deposition rate or the Hall mobility were not found.

The electrical properties, i.e., the electrical resistivity, the carrier concentration, and the Hall mobility, were estimated as a function of deposition rate. The carrier concentration was slightly decreased from 1.3 to 1.1 cm<sup>-3</sup> as the deposition rate was increased from 1.2 to 27.4 nm min<sup>-1</sup> although the aluminum content was almost unchanged in this deposition rate range. On the contrary, the Hall mobility was considerably decreased from 34 to 23 cm<sup>2</sup> V<sup>-1</sup> s<sup>-1</sup> as the deposition rate was increased in the same range. As a result, the resistivity was increased from 1.4 to 3.0 × 10<sup>-4</sup> Ω cm.

Upon the detailed consideration about the variation of structural characteristics of the films with a deposition rate, we obtained the following conclusions:

(1) The films deposited on the (11 $\bar{2}$ 0) oriented sapphire substrates heated to 200 °C with a deposition rate in the range 0.7–27.4 nm min<sup>-1</sup> were (0001) oriented single-crystalline films but, in those films, there was an interfacial stress caused by atomic spacing mismatch between the film and the substrate.

(2) A detailed consideration about the variation of lattice constant of the film with a deposition rate found that the interfacial stress in the film was compressive, i.e., that the network spacing of atoms at the substrate surface was smaller than the corresponding value for the film.

(3) As a result, the films deposited with considerably larger deposition rates were divided into a mosaic structure in order to suppress the increase in the internal energy of the film as the film thickness was increased, and thus the carrier concentration as well as the Hall mobility were decreased and the resistivity was increased as the deposition rate was increased.

Last, as the resistivities in the range 1.4–3.0 × 10<sup>-4</sup> Ω cm obtained with films grown at 200 °C with a deposition rate ranging from 1.2 to 27.4 nm min<sup>-1</sup> are comparable to those for ITO films, we consider that ZnO:Al films can be practically used as transparent conducting films in the near future.

## ACKNOWLEDGMENTS

One of the authors (Y.I.) wishes to thank Dr. K. Murakami for helpful advice about SEM observations and WDS measurements. He also wishes to express his appreciation to the Takahashi Foundation for their financial support.

- <sup>1</sup>T. Minami, H. Nanto, and S. Takata, *Jpn. J. Appl. Phys.* **23**, L280 (1984).
- <sup>2</sup>D. Raviendra and J. K. Sharma, *J. Appl. Phys.* **58**, 838 (1985).
- <sup>3</sup>S. Takata, T. Minami, and H. Nanto, *Thin Solid Films* **135**, 183 (1986).
- <sup>4</sup>Z.-C. Jin, I. Hamberg, and C. G. Granqvist, *Appl. Phys. Lett.* **51**, 149 (1987).
- <sup>5</sup>Y. Igasaki, M. Ishikawa, and G. Shimaoka, *Appl. Surf. Sci.* **33/34**, 926 (1988).
- <sup>6</sup>Z.-C. Jin, I. Hamberg, and C. G. Granqvist, *J. Appl. Phys.* **64**, 5117 (1988).
- <sup>7</sup>M. Ruth, J. Tuttle, J. Goral, and R. Noufi, *J. Cryst. Growth* **96**, 363 (1989).
- <sup>8</sup>Y. Igasaki, M. Ishikawa, and G. Shimaoka, *J. Vac. Soc. Jpn.* **30**, 467 (1987).
- <sup>9</sup>E. L. Paradis and A. J. Shuskus, *Thin Solid Films* **38**, 131 (1976).
- <sup>10</sup>Mu-Shiang Wu, A. Azuma, T. Shiosaki, and A. Kawabata, *J. Appl. Phys.* **62**, 2482 (1987).
- <sup>11</sup>T. Mitsuyu, S. Ono, and K. Wasa, *J. Appl. Phys.* **51**, 2646 (1980).
- <sup>12</sup>E. Krikorian and R. J. Sneed, *J. Appl. Phys.* **37**, 3655 (1966).
- <sup>13</sup>Y. Igasaki and H. Saito, *J. Appl. Phys.* **69**, 2190 (1991).
- <sup>14</sup>Y. Igasaki and N. Inoue, *J. Vac. Soc. Jpn.* **32**, 301 (1989).
- <sup>15</sup>G. Neumann, in *Current Topics in Materials Science*, edited by E. Kaldis (North Holland, Amsterdam, 1981), Vol. 7, p. 154.
- <sup>16</sup>Y. Igasaki and H. Saito, *Extended Abstracts of the 50th Autumn Meeting* (The Japan Society of Applied Physics, Fukuoka, 1989), p. 430.
- <sup>17</sup>P. Ponasewicz, R. Littbarski, and M. Grunze, in *Current Topics in Materials Science*, edited by E. Kaldis (North Holland, Amsterdam, 1981), Vol. 7, p. 371.
- <sup>18</sup>H. Saito and Y. Igasaki, *J. Vac. Soc. Jpn.* **34**, 331 (1991).
- <sup>19</sup>N. Ito and K. Okamoto, *Oyo Butsuri* **57**, 353 (1988).